Hyperfine interactions
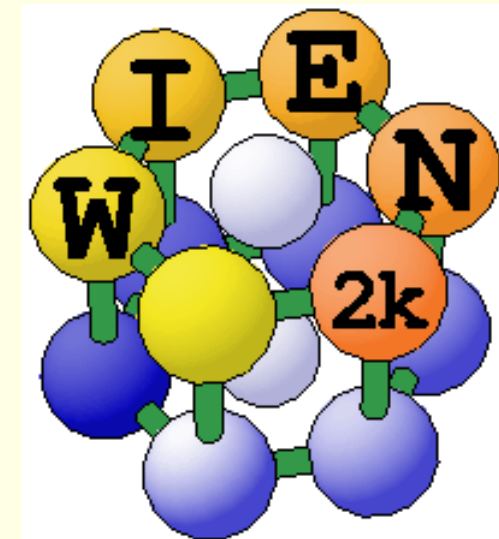
Mössbauer, PAC and NMR Spectroscopy:
Quadrupole splittings, Isomer shifts, Hyperfine fields (~~NMR shifts~~)

Peter Blaha

Institute of Materials Chemistry

TU Wien

hyperfine interaction

=

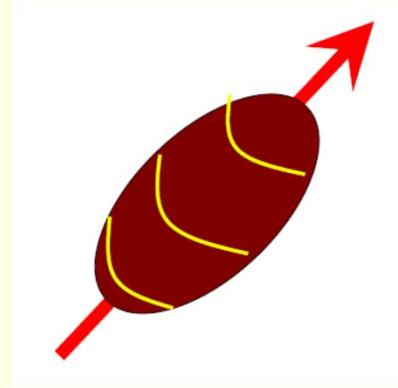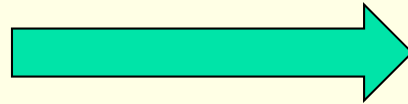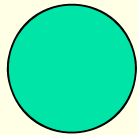**all aspects of the nucleus-electron interaction which go beyond an electric point charge for a nucleus**
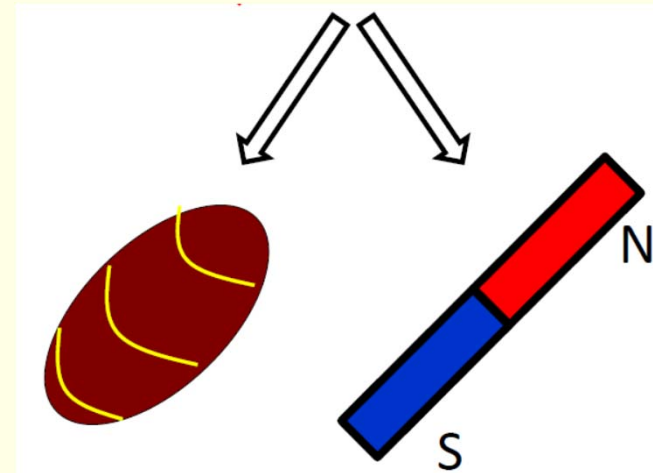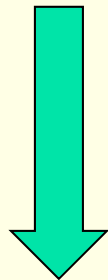
and is

measured at the nucleus

(affects the nucleus)

description of the nucleus:

electric point charge (Z/r)

nucleus with volume, shape and magnetic moment

- **NMR**
- **NQR**
- **Mössbauer spectroscopy**
- **TDPAC**

Electric Hyperfine-Interaction

■ between nuclear charge distribution (σ) and external potential

$$E = \int \sigma_n(x) V(x)\, dx$$

■ Taylor-expansion at the nuclear position

$$E = V_0 Z$$

direction independent constant
(monopole interaction)

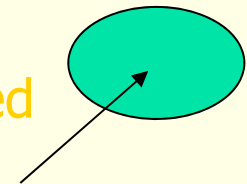$$+ \sum_i \frac{\partial V(0)}{\partial x_i} \int \sigma(x)\, x_i\, dx$$

electric field   x
nuclear dipol moment (=0)

$$+ \frac{1}{2} \sum_{ij} \frac{\partial^2 V(0)}{\partial x_i \partial x_j} \int\int \sigma(x)\, x_i\, x_j\, dx$$

electric fieldgradient x
nuclear quadrupol moment Q

$$+ \ldots$$

higher terms neglected

nucleus with charge Z, but not a sphere

- **Mössbauer Isomer Shift δ:**
  - *integral over nuclear radius of electron density x nuclear charge*
  - *nuclear radii are different for ground and excited state*

$$\delta = \Delta E_A - \Delta E_Q$$

$$= \left(\rho_A(0) - \rho_Q(0)\right)\left(R_A^2 - R_Q^2\right)$$

$$= \alpha\left(\rho_A(0) - \rho_Q(0)\right)$$

α (^{57}Fe)=-0.24 mm/s a_0^3

→ large $\rho_A(0)$→ neg. IS

Fe^{2+}, Fe^{3+},...

:RTOxxx = $\rho(0)$

bcc Fe

Fe(I) S=3/2
Fe(I) S=1/2
Fe(II) S=2
Fe(II) S= 1
Fe(II) S=0
Fe(III) S=5/2
Fe(III) S=3/2
Fe(III) S=1/2
Fe(IV) S=2
Fe(VI) S=1   Fe(IV) S= 1

δ /mms^{-1}
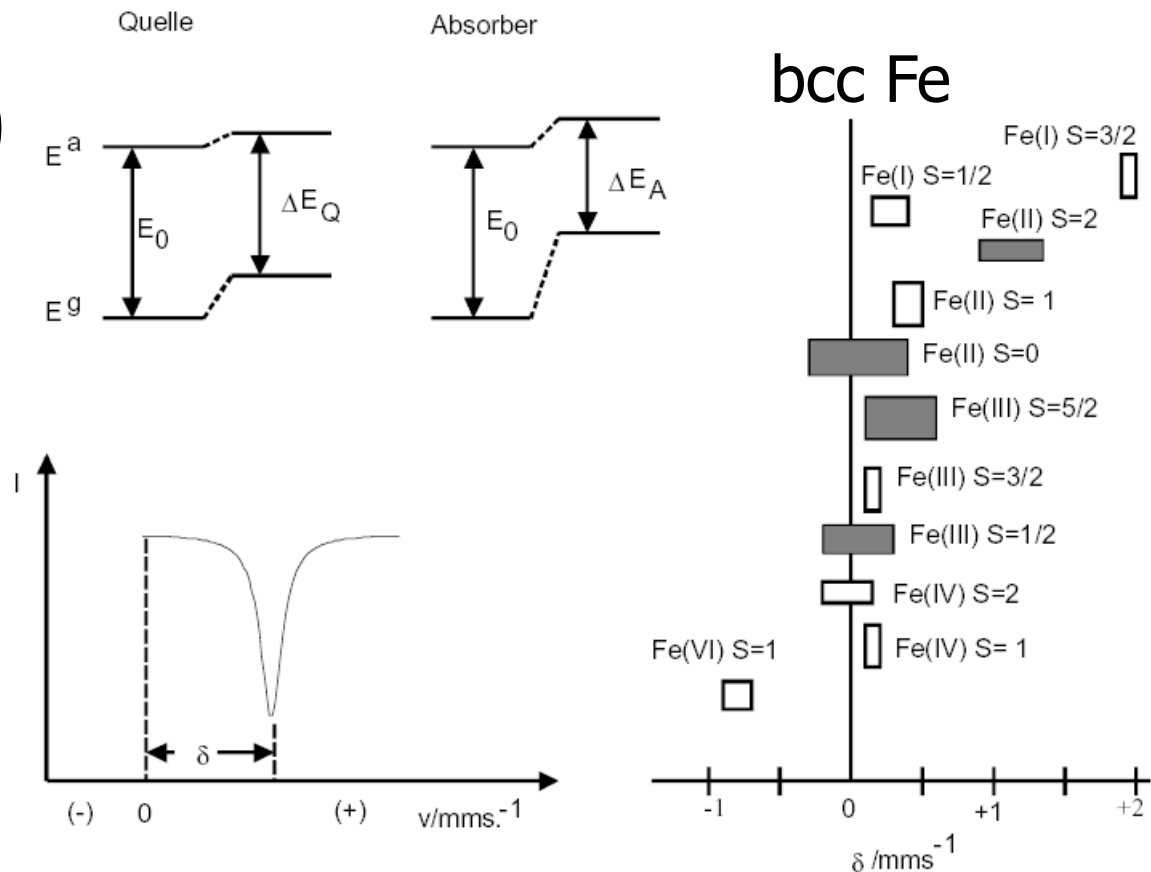
Quadrupole interaction

$$E = \frac{1}{2} \sum_{ij} V_{ij} \, Q$$

$Q(^{57}Fe)=0.16$ barn

V_{ij}: traceless 3x3 tensor of **electric field gradient** EFG (2nd derivative of V(0))

similarity transformation

$$\begin{vmatrix} V_{aa} & V_{ab} & V_{ac} \\ V_{ba} & V_{bb} & V_{bc} \\ V_{ca} & V_{cb} & V_{cc} \end{vmatrix} \Rightarrow \begin{vmatrix} V_{xx} & 0 & 0 \\ 0 & V_{yy} & 0 \\ 0 & 0 & V_{zz} \end{vmatrix}$$
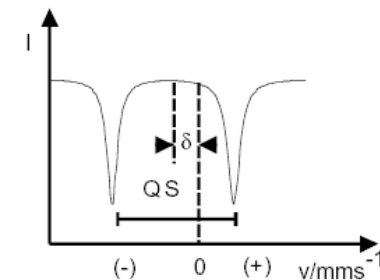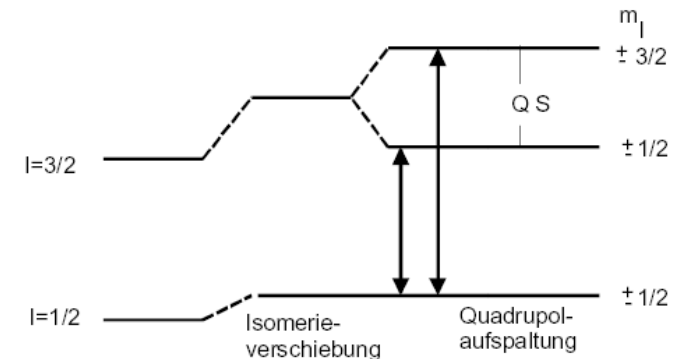
with

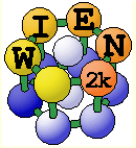$$V_{xx} + V_{yy} + V_{zz} = 0$$

$$|V_{zz}| \geq |V_{yy}| \geq |V_{xx}|$$

$$V_{ij} = \frac{\partial^2 V(0)}{\partial x_i \partial x_j}$$

EFG characterized by principal component V_{zz} and asymmetry parameter η

$$\eta = \frac{/V_{xx}/ - /V_{yy}/}{/V_{zz}/}$$

$$QS = \frac{1}{2} eQV_{zz} \sqrt{1 + \frac{\eta^2}{3}}$$

First-principles calculation of EFG

First-Principles Calculation of the Electric Field Gradient of Li_3N

P. Blaha and K. Schwarz

Institut für Technische Elektrochemie, Technische Universität Wien, A-1060 Vienna, Austria

and

P. Herzig

Institut für Physikalische Chemie, Universität Wien, A-1090 Vienna, Austria

(Received 5 December 1984)

N
Li(1)
Li(2)
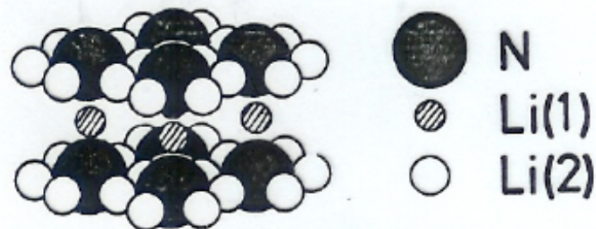
Fig. 1. Crystal structure of Li_3N with increased c dimension
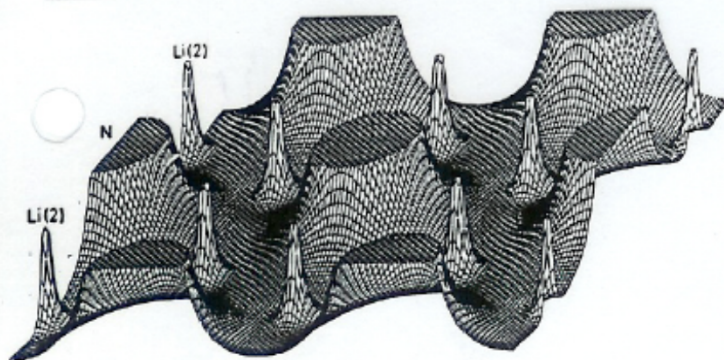
TABLE I. Electric field gradient Φ_{zz} in 10^{20} V m^{-2}.

Model for Φ_{zz}	Li(1)	Li(2)	Li(1)/Li(2)	N
Point charge	−20.37	9.01	2.26	0.33
Muffin-tin LAPW	−7.47	3.72	2.00	3.41
Present work	−6.94	3.41	2.04	11.16
Experiment	−5.87	2.88	2.04	13.04

Previous: point charge model and
Sternheimer factor to experimental value
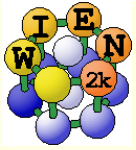
Determination of the Nuclear Quadrupole Moment of ^{57}Fe

Philipp Dufek, Peter Blaha, and Karlheinz Schwarz

Institut für Technische Elektrochemie, Technische Universität Wien, A-1060 Vienna, Austria

(Received 17 July 1995)

$$E = \frac{1}{2} \sum_{ij} V_{ij} Q$$

Theoretical and experimental Fe-EFG in Fe-compounds
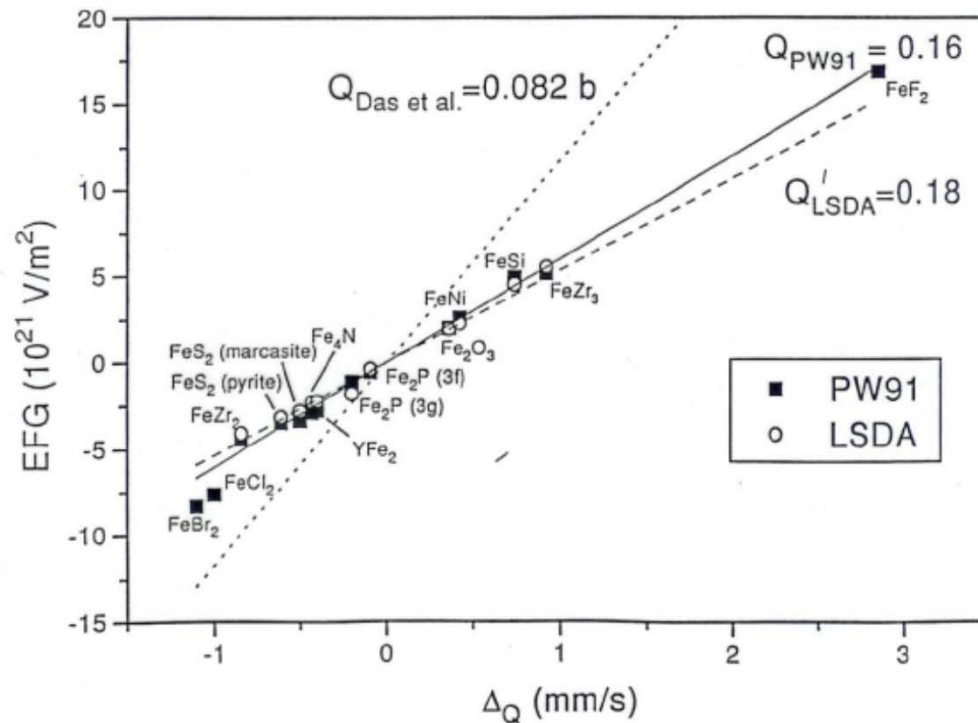
- From the slope between
  - *the theoretical EFG and*
  - *experimental quadrupole splitting Δ_Q (mm/s)*
- the nuclear quadrupole moment Q of the most important Mössbauer nucleus is found to be about twice as large (Q=0.16 b) as so far in literature (Q=0.082 b)

We write the charge density and the potential inside the atomic spheres in a lattice-harmonics expansion

$$\rho(r) = \sum_{LM} \rho_{LM}(\bar{r}) Y_{LM}(\hat{r}); \quad V_{ij} = \frac{\partial^2 V(0)}{\partial x_i \partial x_j}; \quad V_c(r) = \int \frac{\rho(r')}{r - r'} dr'$$

spatial decomposition :

$$V_{zz} \propto \int \frac{\rho(r) Y_{20}}{r^3} d^3r = \int_{sphere} \frac{\sum_{LM} \rho_{LM}(r) Y_{LM} Y_{20}}{r^3} d^3r + \int_{interstital} \frac{\rho(r) Y_{20}}{r^3} d^3r$$

$$V_{zz} \propto \qquad = \int_{sphere} \frac{\rho_{20}(r)}{r^3} dr + interstitial$$

orbital decomposition :

$$\rho_{20}(r) = \int \sum_{k,n.l,l',m,m'} \phi_{lm}^{nk^*} \phi_{l'm'}^{nk} Y_{20} \, d\hat{r} \quad \Rightarrow \quad p-p; d-d; (s-d) \, contr.$$

$$V_{zz} = V_{zz}^{pp} + V_{zz}^{dd} + ... + \quad interstitial$$

theoretical EFG calculations

$$V_{zz} = V_{zz}^{pp} + V_{zz}^{dd} + \ldots + \textit{interstitial}$$

$$V_{zz}^{pp} \propto \left\langle \frac{1}{r^3} \right\rangle_p \left[\frac{1}{2}(p_x + p_y) - p_z \right]$$

$$V_{zz}^{dd} \propto \left\langle \frac{1}{r^3} \right\rangle_d \left[d_{xy} + d_{x^2-y^2} - \frac{1}{2}(d_{xz} + d_{yz}) - d_{z^2} \right]$$

- EFG is **propartial** to **differences of orbital occupations** , e.g. between p_x, p_y and p_z.
- if these occupancies are the same by symmetry (cubic): **$V_{zz}=0$**
- with "axial" (hexagonal, tetragonal) symmetry ($p_x=p_y$): η**=0**

In the following various examples will be presented.

# EFG (10^{21} V/m^2) in YBa$_2$Cu$_3$O$_7$
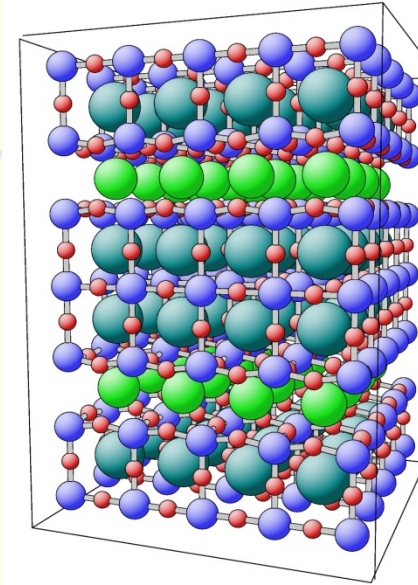
Site		Vxx	Vyy	Vzz	η
Y	theory	-0.9	2.9	-2.0	0.4
	exp.	-	-	-	-
Ba	theory	-8.7	-1.0	9.7	0.8
	exp.	8.4	0.3	8.7	0.9
Cu(1)	theory	-5.2	6.6	-1.5	0.6
	exp.	7.4	7.5	0.1	1.0
Cu(2)	theory	2.6	2.4	-5.0	0.0
	exp.	6.2	6.2	12.3	0.0
O(1)	theory	-5.7	17.9	-12.2	0.4
	exp.	6.1	17.3	12.1	0.3
O(2)	theory	12.3	-7.5	-4.8	0.2
	exp.	10.5	6.3	4.1	0.2
O(3)	theory	-7.5	12.5	-5.0	0.2
	exp.	6.3	10.2	3.9	0.2
O(4)	theory	-4.7	-7.1	11.8	0.2
	exp.	4.0	7.6	11.6	0.3

standard LDA calculations give
good EFGs for all sites except Cu(2)

K.Schwarz, C.Ambrosch-Draxl, P.Blaha, Phys.Rev. B42, 2051 (1990)

D.J.Singh, K.Schwarz, K.Schwarz, Phys.Rev. B46, 5849 (1992)
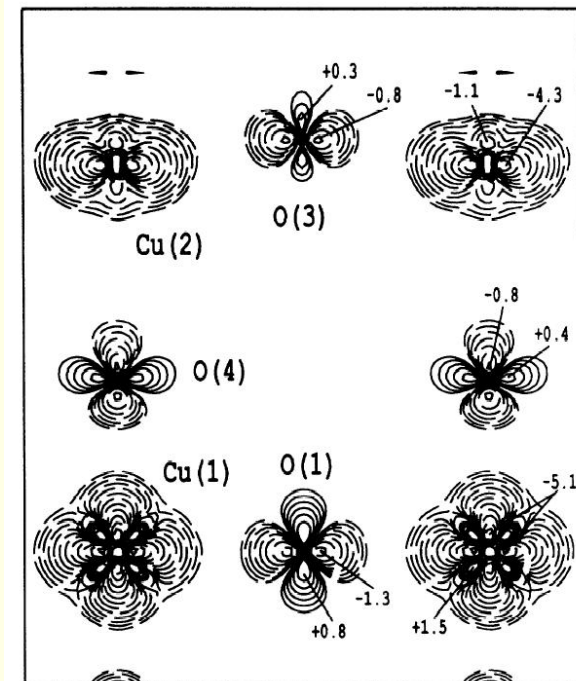
EFG in $YBa_2Cu_3O_7$

- **Interpretation of the EFG at the oxygen sites**

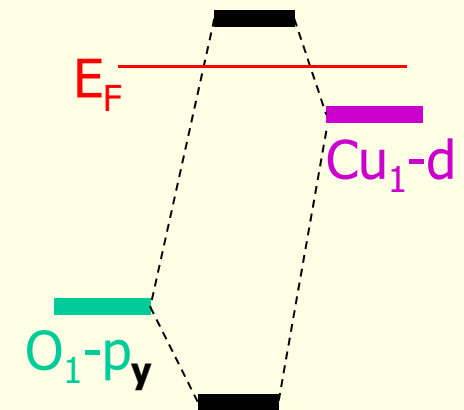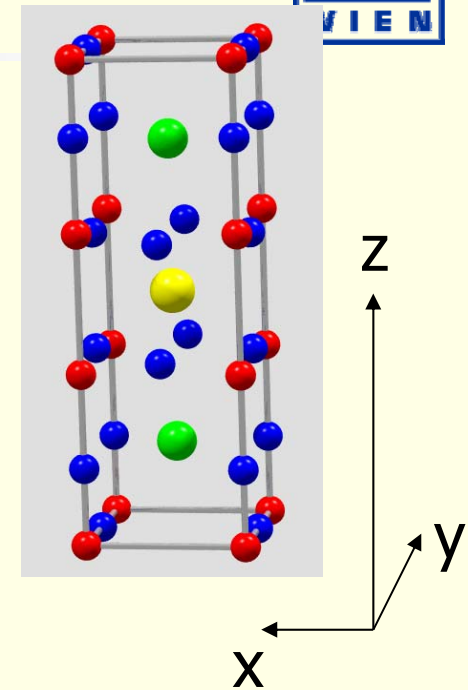|	p_x	p_y	p_z	V_{aa}	V_{bb}	V_{cc}
O(1)	1.18	**0.91**	1.25	-6.1	**18.3**	-12.2
O(2)	**1.01**	1.21	1.18	**11.8**	-7.0	-4.8
O(3)	1.21	**1.00**	1.18	-7.0	**11.9**	-4.9
O(4)	1.18	1.19	**0.99**	-4.7	-7.0	**11.7**

Asymmetry count   **EFG** (p-contribution)

$$\Delta n_p = p_z - \frac{1}{2}(p_x + p_y)$$

$$V_{zz}^p \propto \Delta n_p < \frac{1}{r^3} >_p$$

EFG is proportional to asymmetric charge distribution around given nucleus

z

y

x

E_F

Cu_1-d

O_1-$p_\mathbf{y}$

partly occupied

Cu partial charges in YBa$_2$Cu$_3$O$_7$

	p_x	p_y	p_z	d_{z^2}	$d_{x^2-y^2}$	d_{xy}	d_{xz}	d_{yz}
Cu(1)	0.03	0.07	0.10	1.41	1.65	1.84	1.84	1.86
Cu(2)	0.07	0.07	0.03	1.76	1.44	1.85	1.82	1.82

0.07 e

$$V_{zz}^p \propto \Delta n_{p_z} \langle \frac{1}{r^3} \rangle_p$$

$$\Delta n_{p_z} = 1/2\,(p_x + p_y) - p_z$$

$$V_{zz}^d \propto \Delta n_d \langle \frac{1}{r^3} \rangle_d$$

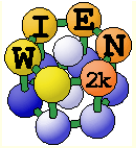$$\Delta n_d = (d_{xy} + d_{x^2-y^2}) - 1/2\,(d_{xz} + d_{yz}) - d_{z^2}$$

$$V_{zz}^p = 0.038 \times 250 = 9.5\ (10^{21}\ V/m^2)$$

$$V_{zz}^d = -.288 \times 47 = -13.5$$

a transfer of **0.07 e** into the $d_z{}^2$ would **increase** the **EFG** from **-5.0** by

$$V_{zz}^d = -.14 \times 47 = -6.6$$

bringing it to **-11.6** inclose to the Experimental value (**-12.3** 10^{21} V/m^2)

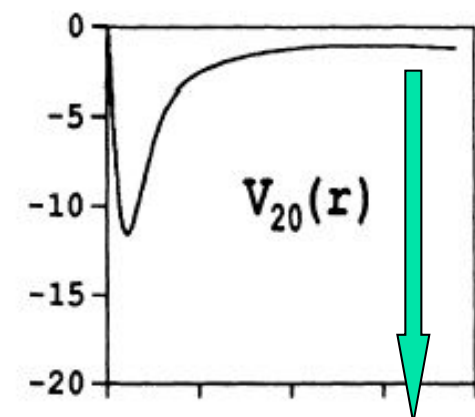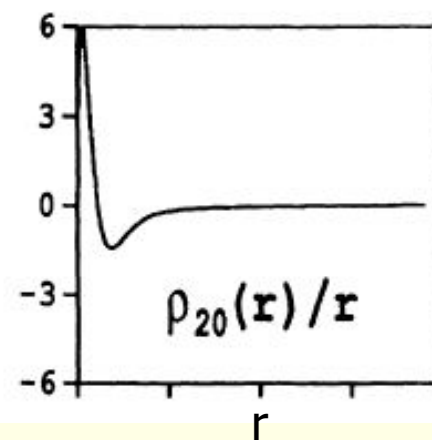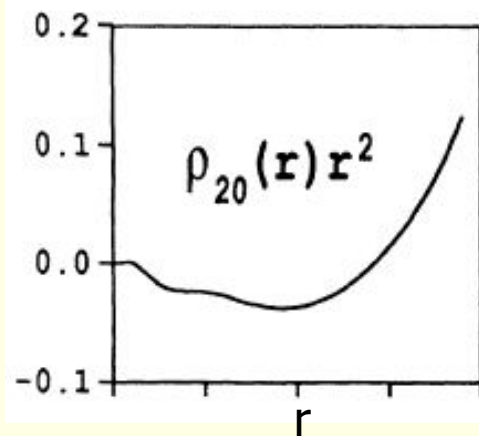- EFG is determined by the non-spherical charge density inside sphere

$$\rho(r) = \sum_{LM} \rho_{LM}(r) Y_{LM} \qquad V_{zz} \propto \int \frac{\rho(r) Y_{20}}{r^3} dr \quad = \quad \int \rho_{20}(r) \, r \, dr$$

- Cu(2)

- O(4)

final EFG
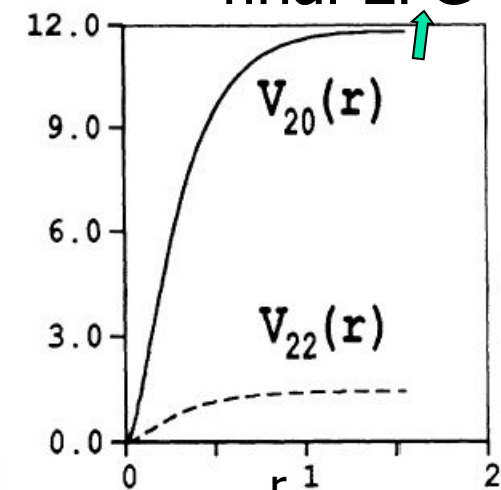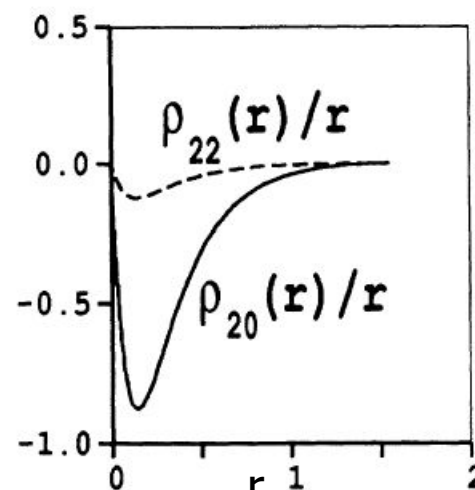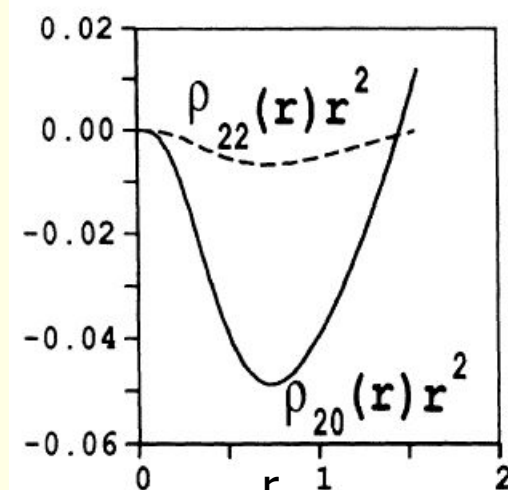
EFG contributions:

- **Depending on the atom, the main EFG-contributions come from anisotropies (in occupation or wave function)**
  - *semicore p-states (eg. Ti 3p much more important than Cu 3p)*
  - *valence p-states (eg. O 2p or Cu 4p)*
  - *valence d-states (eg. TM 3d,4d,5d states; in metals "small")*
  - *valence f-states (only for "localized" 4f,5f systems)*
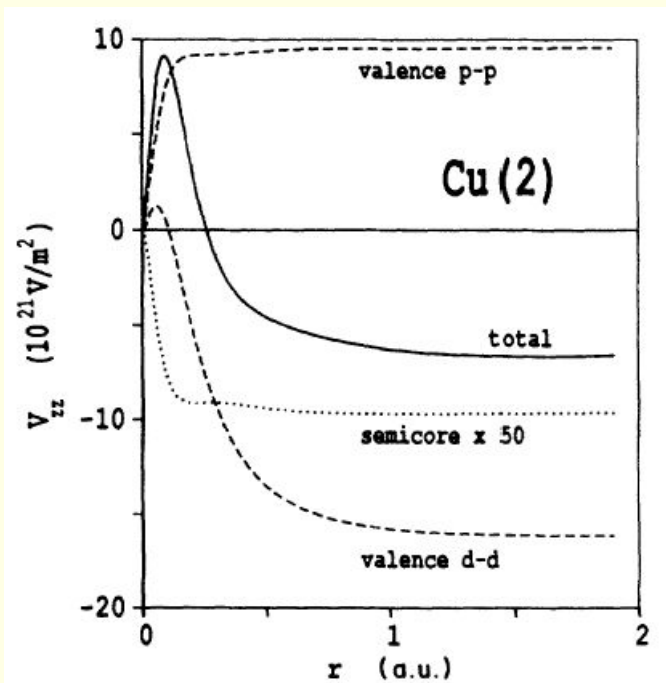
usually only contributions within the first node or within 1 bohr are important.
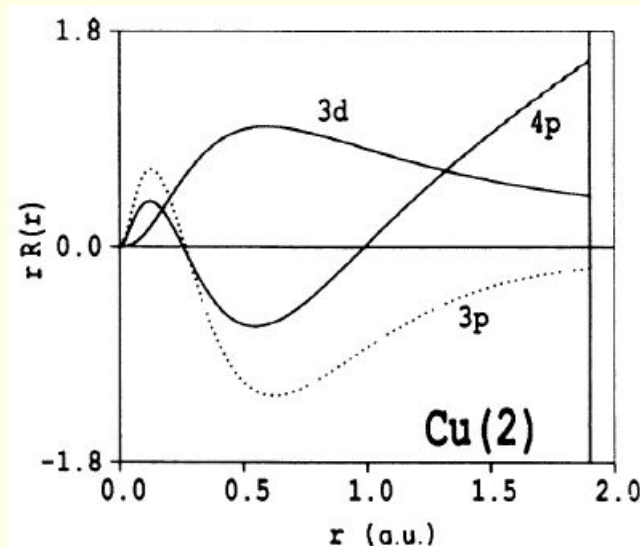
- Undoped Cuprates (La_2CuO_4, $YBa_2Cu_3O_6$) are nonmagnetic metals instead of antiferromagnetic insulators

- Both, doped and undoped cuprates have a "planar Cu" – EFG which is by a factor of 2-3 too small

- We need a method which giver a better description of correlated 3d electrons: can LDA+U fix these problems ??

AMF La_2CuO_4 FLL
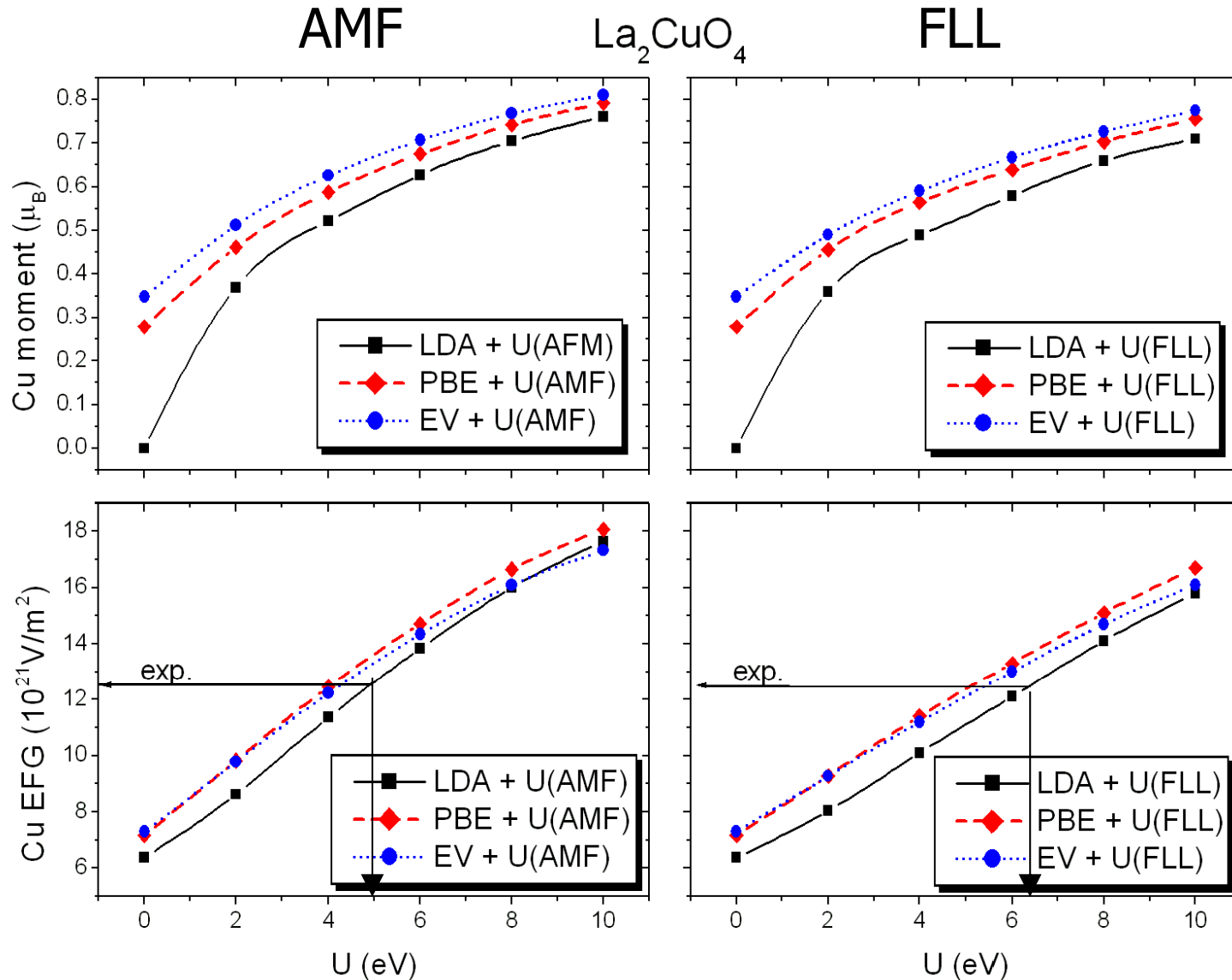
LDA+U gives AF insulator with reasonable moment

U of 5-6 eV gives exp. EFG

GGAs "mimic" a U of 1-2 eV
(EV-GGA more effective than PBE, but very bad E-tot !!)

EFGs in fluoroaluminates

10 different phases of known structures from CaF_2-AlF_3, BaF_2-AlF_3 binary systems and CaF_2-BaF_2-AlF_3 ternary system

Isolated chains of octahedra linked by corners

α-BaAlF$_5$

α-CaAlF$_5$, β-CaAlF$_5$,

β-BaAlF

Isolated octahedra

α-BaCaAlF$_7$

Ca$_2$AlF$_7$, Ba$_3$AlF$_9$-Ib,
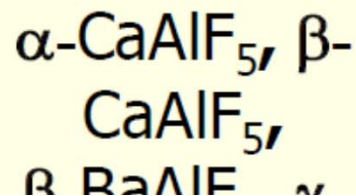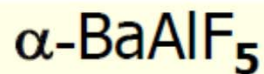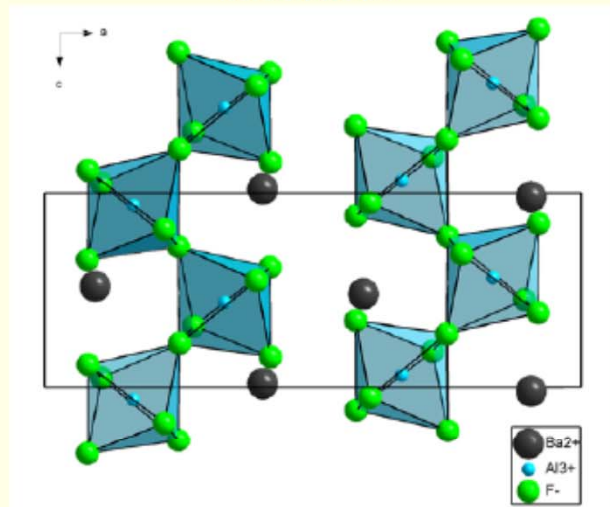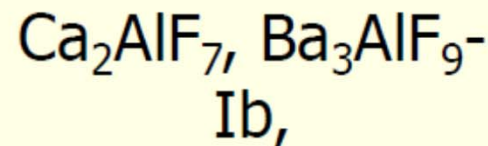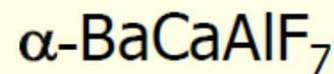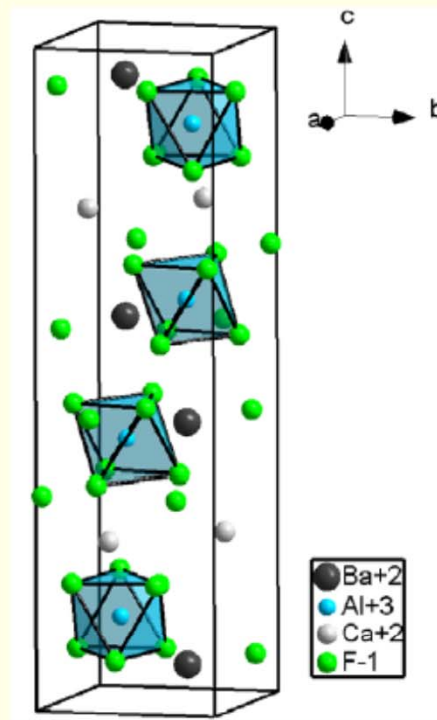
Rings formed by four octahedra sharing corners

Ba$_3$Al$_2$F$_{12}$
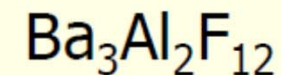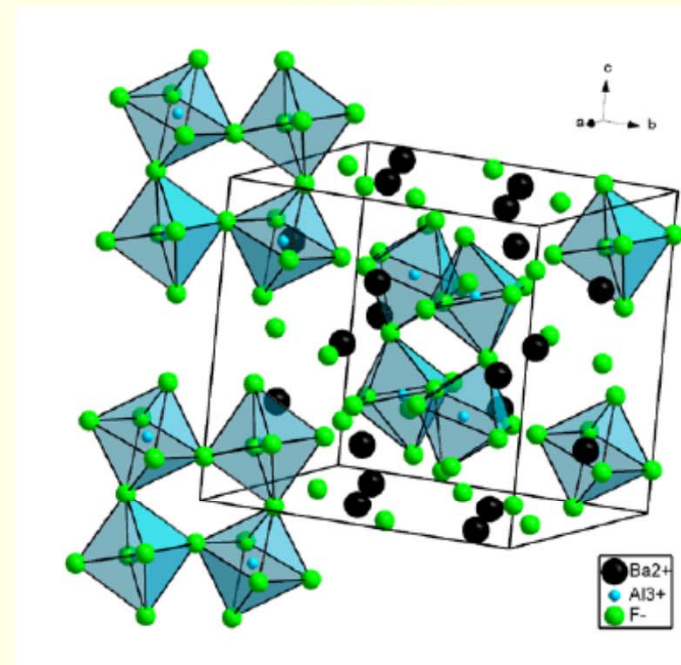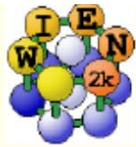
ν_Q and η_Q calculations **using XRD data**

$$\nu_Q = 4{,}712.10^{-16} \; |V_{zz}| \text{ with } R^2 = 0{,}77$$

$\eta_{Q,exp} = 0{,}803$

$\eta_{Q,cal} \; R^2 = 0{,}38$
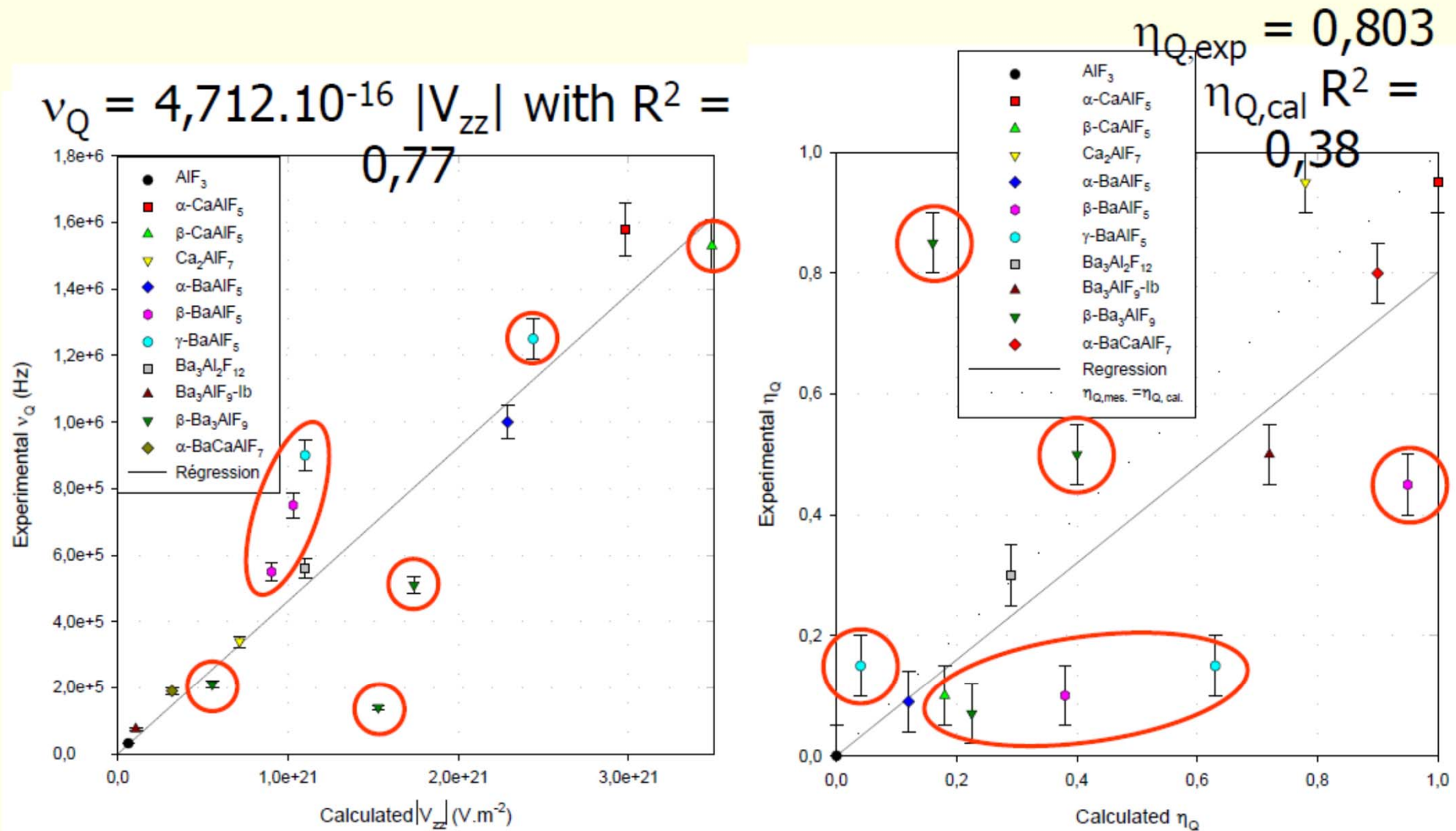
Important discrepancies when structures are used which were determined from X-ray powder diffraction data

ν_Q and η_Q **after structure optimization**

$$\nu_Q = 5{,}85 \cdot 10^{-16} V_{zz}$$
$$R^2 = 0{,}993$$

$$\eta_{Q,\,exp} = 0{,}972\ \eta_{Q,cal}$$
$$R^2 = 0{,}983$$

Legend (left plot):
- ● AlF₃
- ■ α-CaAlF₅
- ▲ β-CaAlF₅
- ▽ Ca₂AlF₇
- ◆ α-BaAlF₅
- ● β-BaAlF₅
- ● γ-BaAlF₅
- □ Ba₃Al₂F₁₂
- ▲ Ba₃AlF₉-Ib
- ▼ β-Ba₃AlF₉
- ◆ α-BaCaAlF₇
- — Regression

Legend (right plot):
- ● AlF₃
- ■ α-CaAlF₅
- ▲ β-CaAlF₅
- ▽ Ca₂AlF₇
- ◆ α-BaAlF₅
- ● β-BaAlF₅
- ● γ-BaAlF₅
- □ Ba₃Al₂F₁₂
- ▲ Ba₃AlF₉-Ib
- ▼ β-Ba₃AlF₉
- ◆ α-BaCaAlF₇
- — Regression
- ···· $\eta_{Q,exp.} = \eta_{Q,\,cal.}$

Left axis: Experimental ν_Q (Hz); x-axis: Calculated $|V_{zz}|$ (V·m⁻²)
Right axis: Experimental η_Q; x-axis: Calculated η_Q

Very fine agreement between experimental and calculated values

M.Body, et al., *J.Phys.Chem. A 2007, 111, 11873*
(Univ. LeMans)

Magnetic hyperfine interaction

- Zeman - interaction between magnetic moment I of the nucleus and the external magnetic field B (at the nucleus, produced by the spin-polarized e⁻ in a FM)

$$B \propto \left(\rho_\uparrow(0) - \rho_\downarrow(0) \right)$$

B proportional to the **spindensity** at the nucleus

B often proportional to the magnetic moment of an atom in a solid.
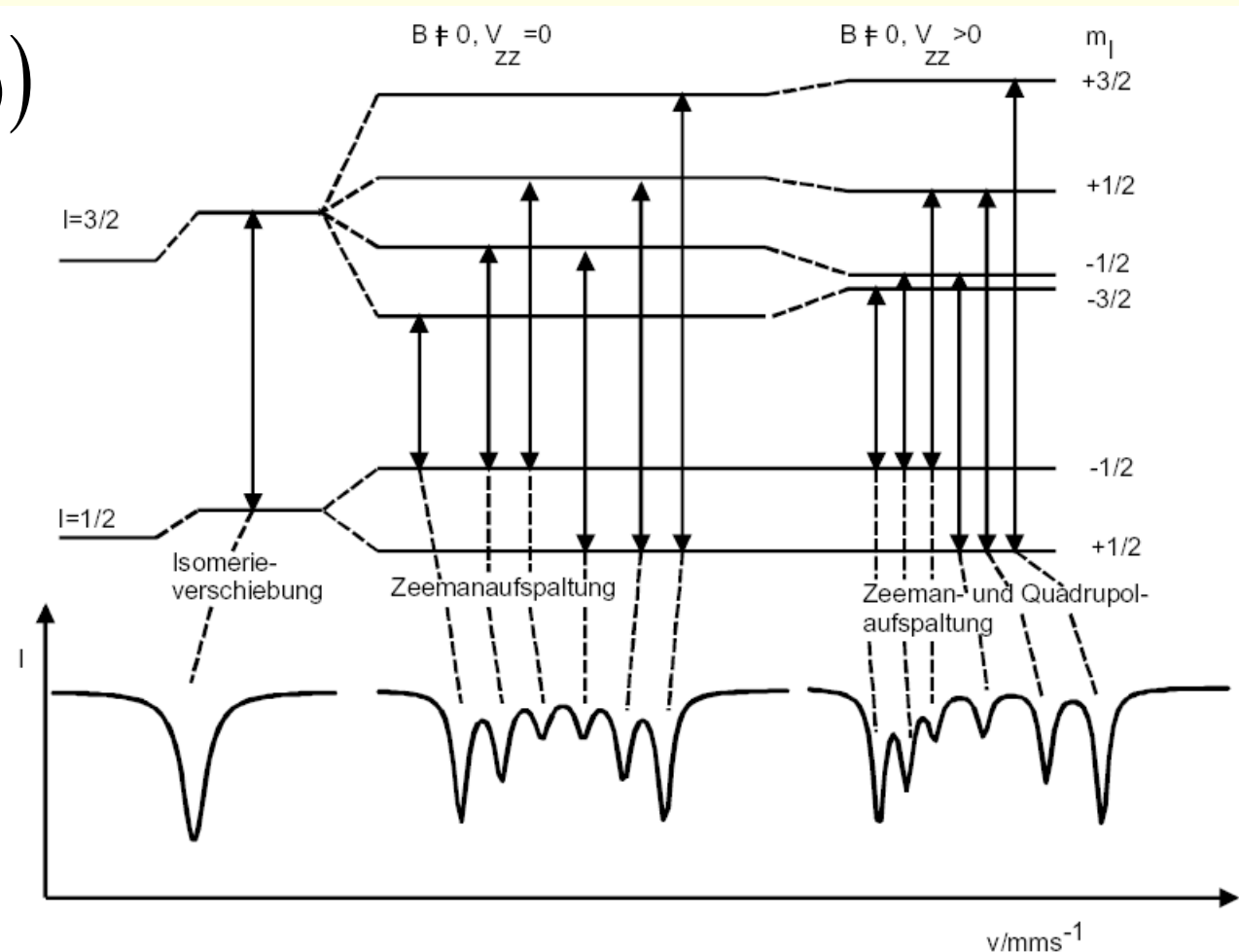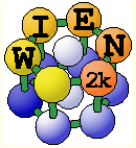
Source of magnetic fields at the nuclear site in an atom/solid

$$B_{tot} = B_{dip} + B_{orb} + B_{fermi} + B_{lat}$$

➤ B_{dip} = electron as bar magnet
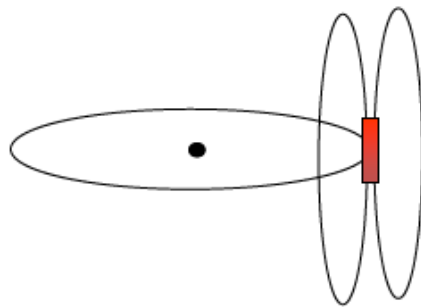
➤ B_{orb} = electron as current loop
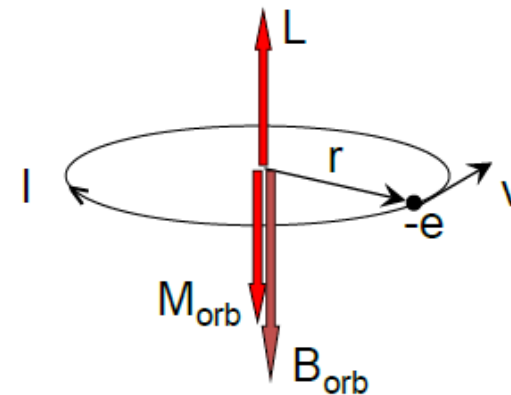
➤ B_{Fermi} = electron in nucleus
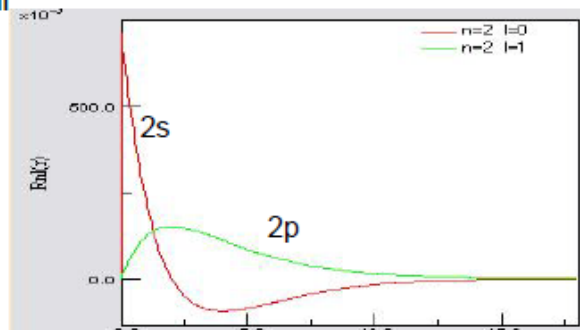
➤ B_{lat} = neighbours as bar magnets

$$-\frac{2\mu_B\mu_0}{3}\left(|\psi_{e,\uparrow}(0)|^2 - |\psi_{e,\downarrow}(0)|^2\right)$$
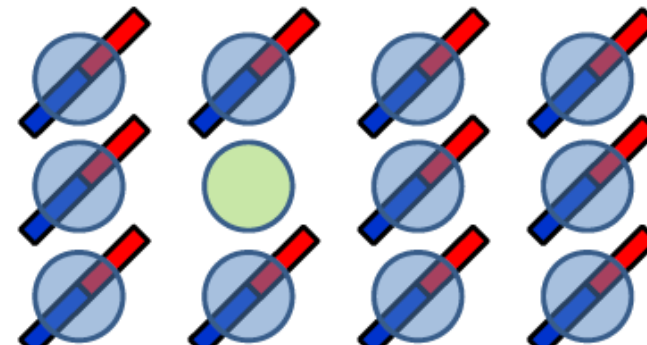
Magnetic fields at the nucleus:
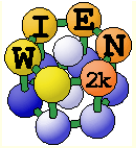
- Magnetic Hyperfine fields: $B_{tot} = B_{contact} + B_{orb} + B_{dip}$

  - $B_{contact} = 8\pi/3 \, \mu_B [\rho_{up}(0) - \rho_{dn}(0)]$ ...   *spin-density at the nucleus*

$$\vec{B}_{orb} = 2\mu_B \langle\Phi| \frac{S(r)}{r^3} \vec{l} |\Phi\rangle$$ ...   *orbital-moment*

$$\vec{B}_{dip} = 2\mu_B \langle\Phi| \frac{S(r)}{r^3} \left[3(\vec{s}\,\hat{\vec{r}})\,\hat{\vec{r}} - \vec{s} \right] |\Phi\rangle$$ *... spin-moment*

S(r) is reciprocal of the relativistic mass enhancement $S(r) = \left[1 + \frac{\epsilon - V(r)}{2mc^2} \right]^{-1}$

Magnetic hyperfine field

In regular scf file:

  :HFFxxx   (Fermi contact contribution)

After post-processing with LAPWDM :

• orbital hyperfine field ("3 3" in case.indmc)
• dipolar hyperfine field ("3 5" in case.indmc)

in case.scfdmup

```
------------------ top of file: case.indm ------------------
-9.                       Emin cutoff energy
1                         number of atoms for which density matrix is calculated
1  1  2         index of 1st atom, number of L's, L1
0  0            r-index, (l,s)-index
------------------ bottom of file ----------------------
```

After post-processing with DIPAN :

• lattice contribution

in case.outputdipan

more info:
UG 7.8 (lapwdm)
UG 8.3 (dipan)

Verwey transition in $YBaFe_2O_5$

charge ordered (CO) phase:

Pmma a:b:c=2.09:1:1.96 (20K)
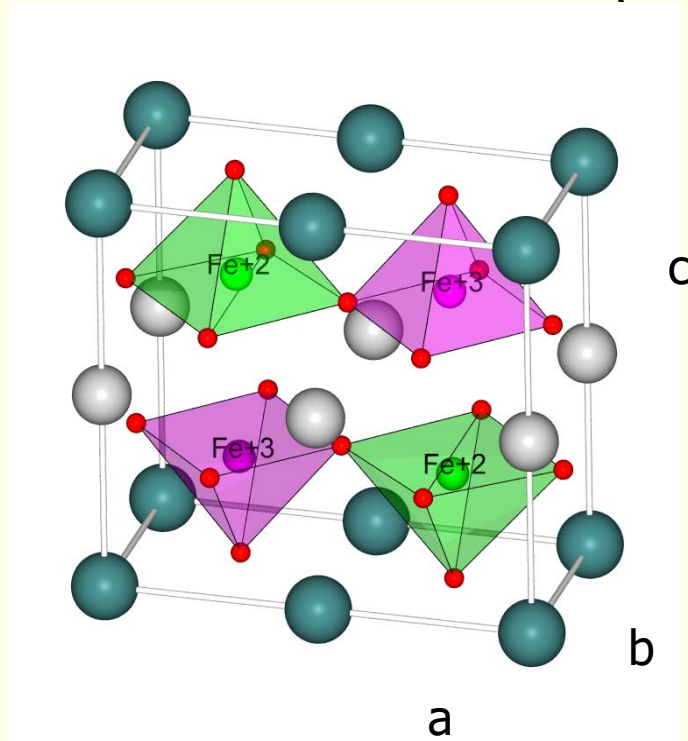
valence mixed (VM) phase:

Pmmm a:b:c=1.003:1:1.93 (340K)
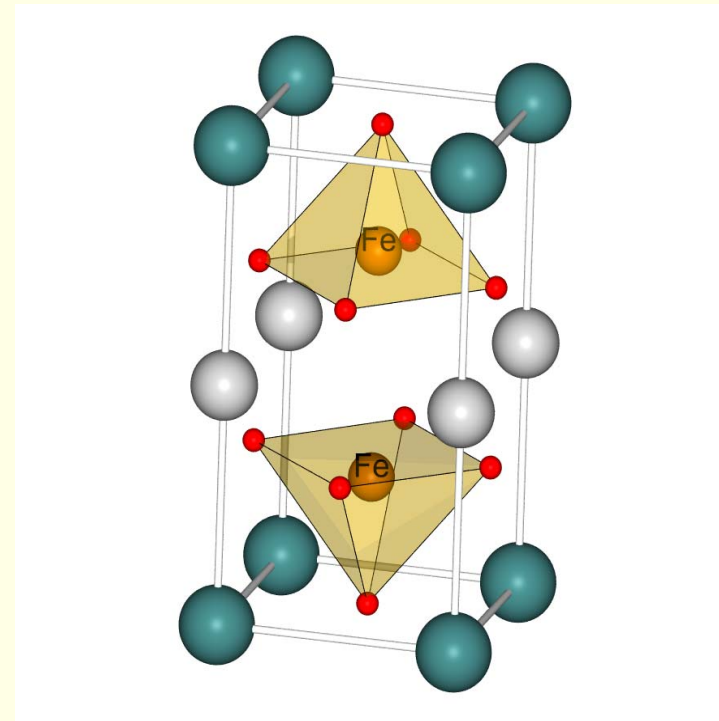
- Fe^{2+} and Fe^{3+} form chains along b
- contradicts Anderson charge-ordering conditions with minimal electrostatic repulsion (checkerboard like pattern)
- has to be compensated by orbital ordering and e^--lattice coupling
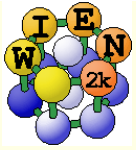
DOS: GGA+U vs. GGA

GGA+U

GGA

single lower Hubbard-band in VM splits in CO with Fe^{3+} states lower than Fe^{2+}
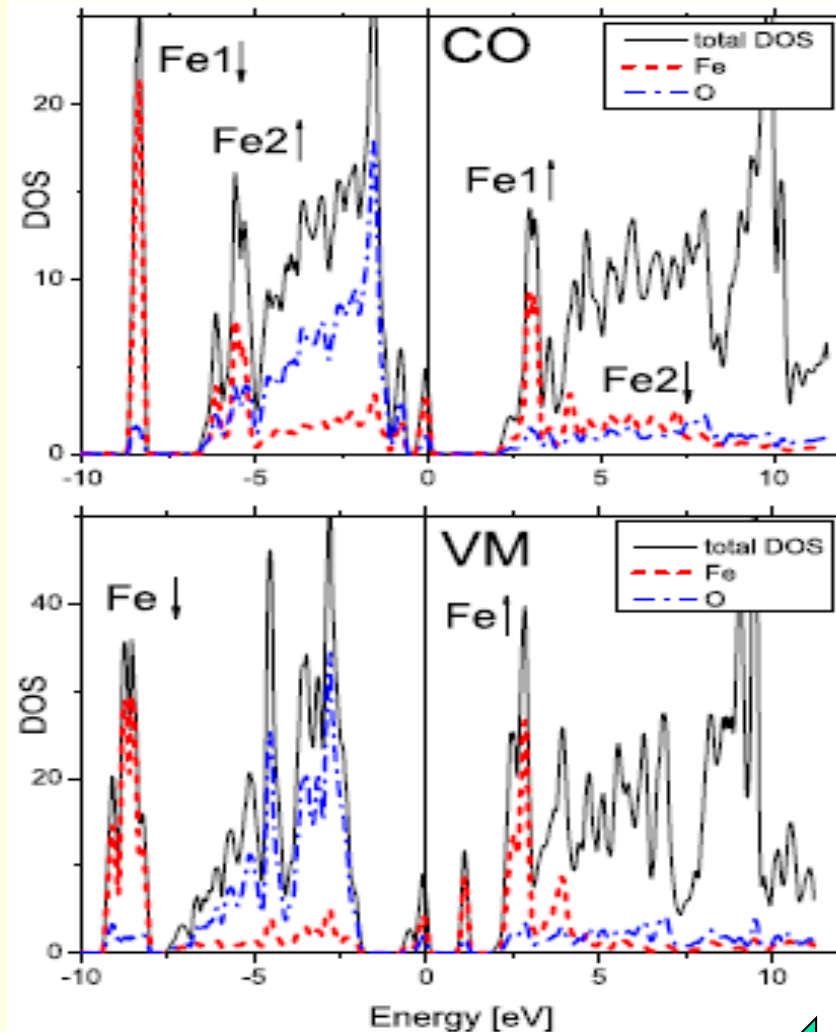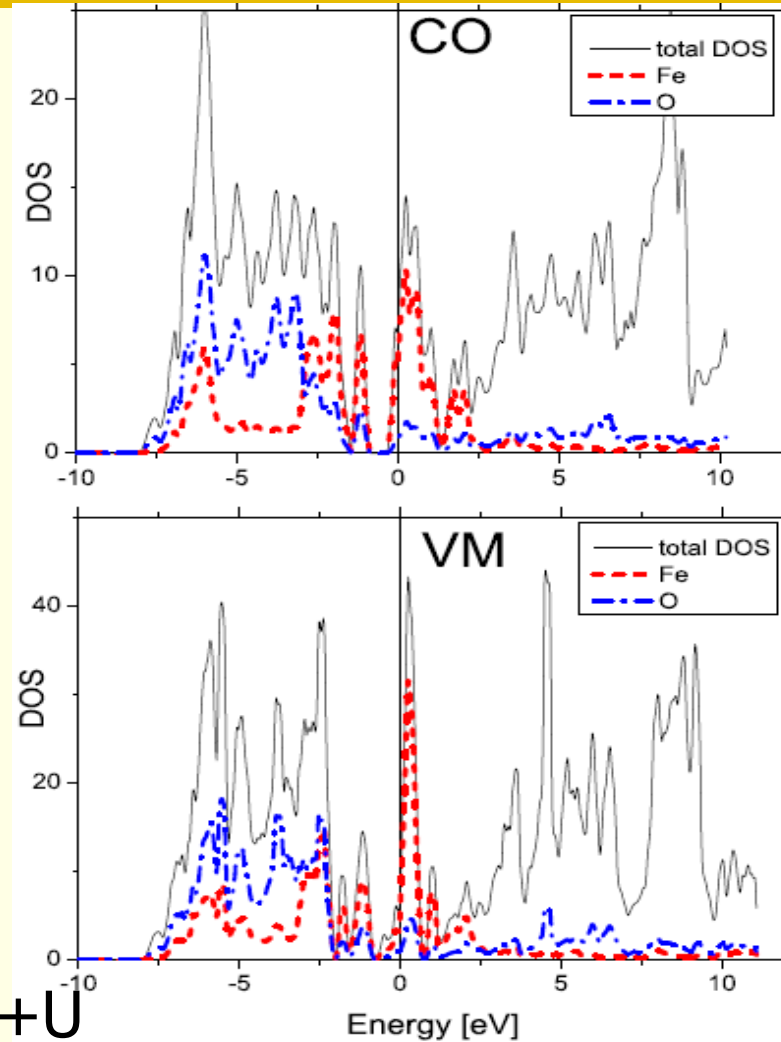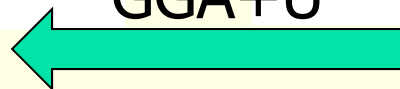
insulator ← GGA+U metal

Difference densities $\Delta\rho = \rho_{cryst} - \rho_{at}^{sup}$

CO phase
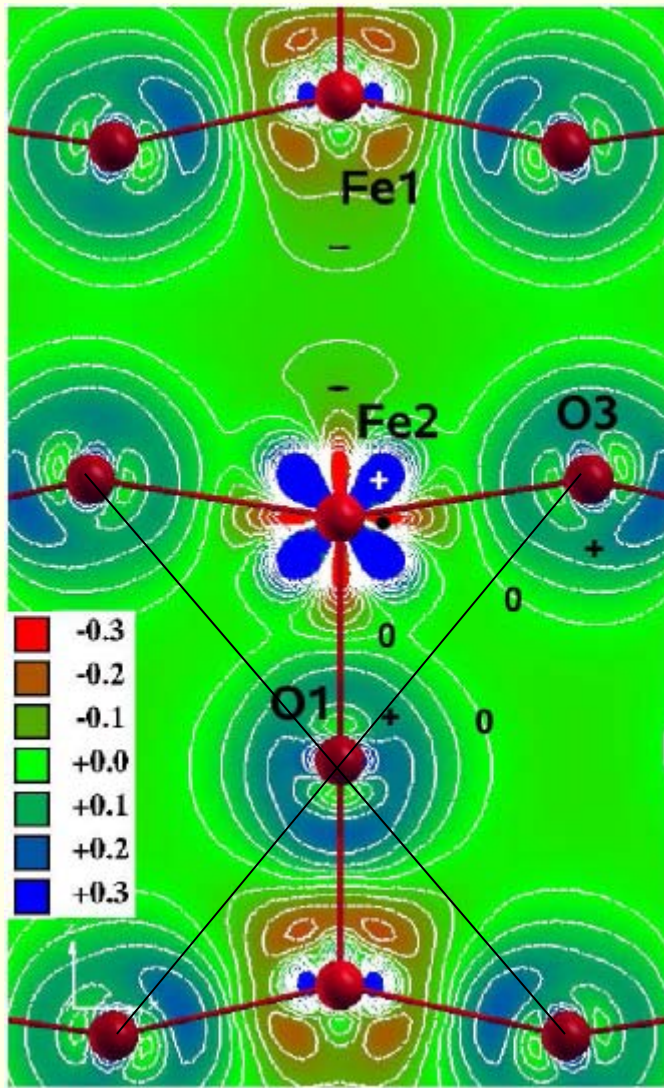
VM phase

Fe^{2+}: d-xz
Fe^{3+}: d-x^2
O1 and O3: polarized
toward Fe^{3+}

Fe: d-z^2 Fe-Fe interaction
O: symmetric
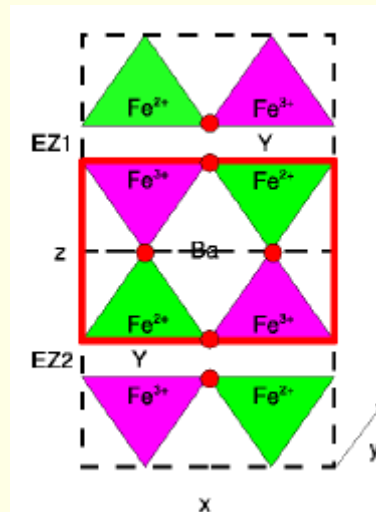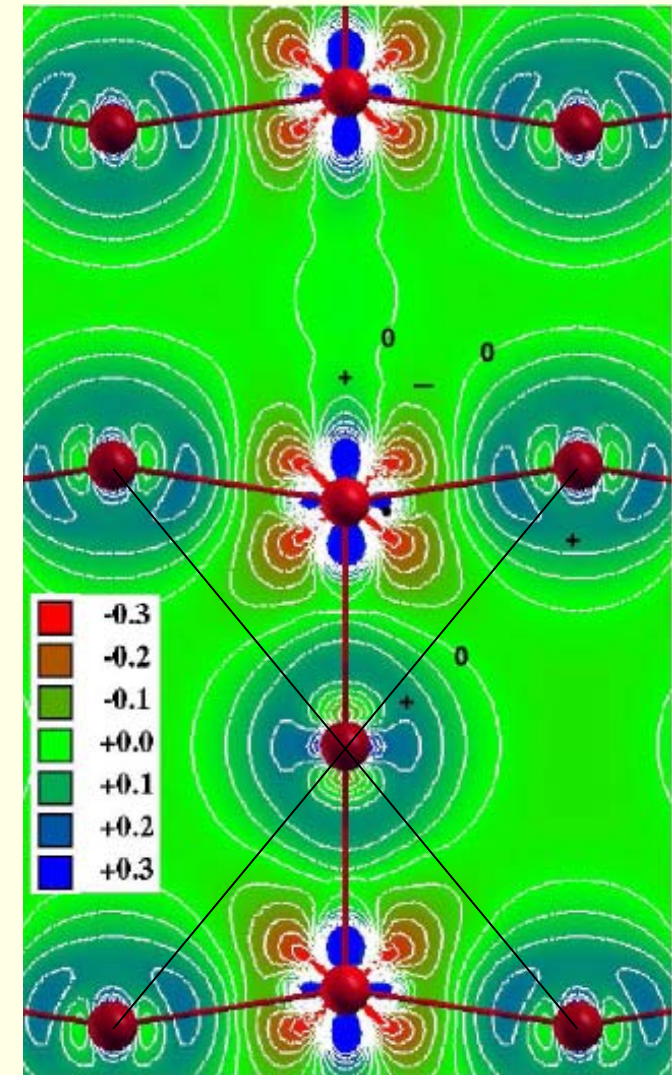
Mössbauer spectroscopy

TABLE VIII: Hyperfine fields B (in Tesla), isomer shifts δ (mm/s) and quadrupole coupling constants eQV_{zz} (mm/s) for the CO phase for various exchange and correlation potentials and experiment[8–10].

CO

		exp.	GGA+U				LDA	GGA
	U_{eff} [eV]	—	5	6	7	8	—	—
Fe2^{2+}	B_{dip}	—	-16.29	-16.49	-16.66	-16.83	-6.68	-12.67
	B_{orb}	—	-6.73	-6.90	-8.26	-7.65	-9.57	-6.34
	$B_{contact}$	—	32.25	32.23	32.58	32.60	32.21	31.58
	B_{tot}	~ 8	9.23	8.83	7.66	8.13	15.96	12.57
	δ	~ 1	0.92	0.94	0.96	0.99	0.74	0.79
	eQV_{zz}	$3.6-4$[a]	3.66	3.74	3.81	3.89	-0.82	2.60
Fe1^{3+}	B_{dip}	—	-0.67	-0.60	-0.52	-0.45	1.29	0.39
	B_{orb}	—	-0.52	-0.45	-0.37	-0.28	-7.96	-2.65
	$B_{contact}$	—	37.65	38.28	38.15	37.86	29.64	31.63
	B_{tot}	~ 50	36.46	37.24	37.26	37.12	22.97	29.37
	δ	~ 0.4	0.33	0.30	0.28	0.25	0.50	0.47
	eQV_{zz}	$1-1.5$[a]	1.46	1.50	1.51	1.52	1.04	-0.30

[a]depending on rare earth ion

VM

		exp.	GGA+U				LDA	GGA
	U_{eff} [eV]	—	5	6	7	8	—	—
Fe$^{2.5+}$	B_{dip}	—	-3.00	-2.98	-2.95	-2.87	-2.13	-2.83
	B_{orb}	—	-3.11	-2.99	-2.84	-2.74	-5.47	-4.56
	$B_{contact}$	—	41.17	40.96	41.45	41.17	33.10	36.36
	B_{tot}	~ 30	35.06	34.98	35.67	35.56	25.50	28.98
	δ	~ 0.5	0.53	0.52	0.51	0.49	0.60	0.60
	eQV_{zz}	~ 0.1	0.12	0.13	0.13	0.13	0.19	-0.27

TABLE VIII: Hyperfine fields B (in Tesla), isomer shifts δ (mm/s) and quadrupole coupling constants eQV_{zz} (mm/s) for the CO phase for various exchange and correlation potentials and experiment[8-10].

CO

		exp.	GGA+U				LDA	GGA
	U_{eff} [eV]	—	5	6	7	8	—	—
Fe2^{2+}	B_{dip}	—	-16.29	-16.49	-16.66	-16.83	-6.68	-12.67
	B_{orb}	—	-6.73	-6.90	-8.26	-7.65	-9.57	-6.34
	$B_{contact}$	—	32.25	32.23	32.58	32.60	32.21	31.58
	B_{tot}	~ 8	9.23	8.83	7.66	8.13	15.96	12.57
	δ	~ 1	0.92	0.94	0.96	0.99	0.74	0.79
	eQV_{zz}	3.6 – 4^a	3.66	3.74	3.81	3.89	-0.82	2.60
Fe1^{3+}	B_{dip}	—	-0.67	-0.60	-0.52	-0.45	1.29	0.39
	B_{orb}	—	-0.52	-0.45	-0.37	-0.28	-7.96	-2.65
	$B_{contact}$	—	37.65	38.28	38.15	37.86	29.64	31.63
	B_{tot}	~ 50	36.46	37.24	37.26	37.12	22.97	29.37
	δ	~ 0.4	0.33	0.30	0.28	0.25	0.50	0.47
	eQV_{zz}	1 – 1.5^a	1.46	1.50	1.51	1.52	1.04	-0.30

^{a}depending on rare earth ion

VM

		exp.	GGA+U				LDA	GGA
	U_{eff} [eV]	—	5	6	7	8	—	—
Fe$^{2.5+}$	B_{dip}	—	-3.00	-2.98	-2.95	-2.87	-2.13	-2.83
	B_{orb}	—	-3.11	-2.99	-2.84	-2.74	-5.47	-4.56
	$B_{contact}$	—	41.17	40.96	41.45	41.17	33.10	36.36
	B_{tot}	~ 30	35.06	34.98	35.67	35.56	25.50	28.98
	δ	~ 0.5	0.53	0.52	0.51	0.49	0.60	0.60
	eQV_{zz}	~ 0.1	0.12	0.13	0.13	0.13	0.19	-0.27

TABLE VIII: Hyperfine fields B (in Tesla), isomer shifts δ (mm/s) and quadrupole coupling constants eQV_{zz} (mm/s) for the CO phase for various exchange and correlation potentials and experiment[8–10].

CO

	U_{eff} [eV]	exp.	GGA+U 5	6	7	8	LDA	GGA
		—	—	—	—	—	—	—
Fe2^{2+}	B_{dip}	—	-16.29	-16.49	-16.66	-16.83	-6.68	-12.67
	B_{orb}	—	-6.73	-6.90	-8.26	-7.65	-9.57	-6.34
	$B_{contact}$	—	32.25	32.23	32.58	32.60	32.21	31.58
	B_{tot}	~ 8	9.23	8.83	7.66	8.13	15.96	12.57
	δ	~ 1	0.92	0.94	0.96	0.99	0.74	0.79
	eQV_{zz}	$3.6 - 4^a$	3.66	3.74	3.81	3.89	-0.82	2.60
Fe1^{3+}	B_{dip}	—	-0.67	-0.60	-0.52	-0.45	1.29	0.39
	B_{orb}	—	-0.52	-0.45	-0.37	-0.28	-7.96	-2.65
	$B_{contact}$	—	37.65	38.28	38.15	37.86	29.64	31.63
	B_{tot}	~ 50	36.46	37.24	37.26	37.12	22.97	29.37
	δ	~ 0.4	0.33	0.30	0.28	0.25	0.50	0.47
	eQV_{zz}	$1 - 1.5^a$	1.46	1.50	1.51	1.52	1.04	-0.30

^{a}depending on rare earth ion

VM

	U_{eff} [eV]	exp.	GGA+U 5	6	7	8	LDA	GGA
		—	—	—	—	—	—	—
Fe$^{2.5+}$	B_{dip}	—	-3.00	-2.98	-2.95	-2.87	-2.13	-2.83
	B_{orb}	—	-3.11	-2.99	-2.84	-2.74	-5.47	-4.56
	$B_{contact}$	—	41.17	40.96	41.45	41.17	33.10	36.36
	B_{tot}	~ 30	35.06	34.98	35.67	35.56	25.50	28.98
	δ	~ 0.5	0.53	0.52	0.51	0.49	0.60	0.60
	eQV_{zz}	~ 0.1	0.12	0.13	0.13	0.13	0.19	-0.27

TABLE VIII: Hyperfine fields B (in Tesla), isomer shifts δ (mm/s) and quadrupole coupling constants eQV_{zz} (mm/s) for the CO phase for various exchange and correlation potentials and experiment[8–10].

CO

		exp.	GGA+U				LDA	GGA
	U_{eff} [eV]	—	5	6	7	8	—	—
$Fe2^{2+}$	B_{dip}	—	-16.29	-16.49	-16.66	-16.83	-6.68	-12.67
	B_{orb}	—	-6.73	-6.90	-8.26	-7.65	-9.57	-6.34
	$B_{contact}$	—	32.25	32.23	32.58	32.60	32.21	31.58
	B_{tot}	~ 8	9.23	8.83	7.66	8.13	15.96	12.57
	δ	~ 1	0.92	0.94	0.96	0.99	0.74	0.79
	eQV_{zz}	$3.6 - 4^a$	3.66	3.74	3.81	3.89	-0.82	2.60
$Fe1^{3+}$	B_{dip}	—	-0.67	-0.60	-0.52	-0.45	1.29	0.39
	B_{orb}	—	-0.52	-0.45	-0.37	-0.28	-7.96	-2.65
	$B_{contact}$	—	37.65	38.28	38.15	37.86	29.64	31.63
	B_{tot}	~ 50	36.46	37.24	37.26	37.12	22.97	29.37
	δ	~ 0.4	0.33	0.30	0.28	0.25	0.50	0.47
	eQV_{zz}	$1 - 1.5^a$	1.46	1.50	1.51	1.52	1.04	-0.30

[a]depending on rare earth ion

VM

		exp.	GGA+U				LDA	GGA
	U_{eff} [eV]	—	5	6	7	8	—	—
$Fe^{2.5+}$	B_{dip}	—	-3.00	-2.98	-2.95	-2.87	-2.13	-2.83
	B_{orb}	—	-3.11	-2.99	-2.84	-2.74	-5.47	-4.56
	$B_{contact}$	—	41.17	40.96	41.45	41.17	33.10	36.36
	B_{tot}	~ 30	35.06	34.98	35.67	35.56	25.50	28.98
	δ	~ 0.5	0.53	0.52	0.51	0.49	0.60	0.60
	eQV_{zz}	~ 0.1	0.12	0.13	0.13	0.13	0.19	-0.27

conversion of exp. data to EFGs

- ## Mössbauer:
  - $\Delta = \{e\, Q\, V_{zz}(1+\eta^2/3)^{1/2}\} / 2$; $\qquad \Delta = (E_\gamma\, \Delta_v) / c$
  - $\Delta_v = (e\, Q\, c\, V_{zz}) / 2\, E_\gamma$ $\qquad Q(^{57}Fe)=0.16\ b;\ E_\gamma =14410\ eV$

  - $Vzz\ [10^{21}\ V/m^2] = 6 * \Delta_v\ [mm/s]$

- ## NMR:
  - $v_Q = (3\, e\, Q\, V_{zz}) / \{2\, h\, I\,(2\, I - 1)\}$ $\qquad I\ ..\ nuclear\ spin\ quantum\ n.$

  - $V_{zz}\ [10^{21}\ V/m^2] = 4.135\ 10^{19}\ v_Q\,[MHz] / Q\ [b]$ $\qquad Q(^{49}Ti)=0.247\ b$